



A Legendrian Thurston–Bennequin bound from Khovanov homology

LENHARD NG

Abstract We establish an upper bound for the Thurston–Bennequin number of a Legendrian link using the Khovanov homology of the underlying topological link. This bound is sharp in particular for all alternating links, and knots with nine or fewer crossings.

AMS Classification 57M27; 57R17, 53D12

Keywords Legendrian link, Thurston–Bennequin number, Khovanov homology, alternating link

1 Introduction

The *standard contact structure* on \mathbb{R}^3 is the two-plane distribution given by the kernel of the one-form $dz - ydx$. A *Legendrian link* in standard contact \mathbb{R}^3 is a link which is everywhere tangent to this contact structure. It is well-known that any topological link type has a Legendrian representative.

To any oriented Legendrian link (or unoriented Legendrian knot), there is an invariant called the *Thurston–Bennequin number*, abbreviated tb , which measures the framing of the contact plane field around the link. Given any Legendrian link, one can construct a Legendrian link in the same topological class but with tb less by 1, by a construction known as stabilization. On the other hand, it is not always possible to increase tb within a link type. A classic result of Bennequin [2] states that tb is bounded above by minus the Euler characteristic of a Seifert surface for the link. The Bennequin bound on tb is one of the fundamental results in three-dimensional contact topology, and implies for example the existence of a contact structure on \mathbb{R}^3 which is homotopic but not isomorphic to the standard one.

Since Bennequin’s result, there has been considerable interest in computing or bounding $\overline{tb}(K)$, the maximal Thurston–Bennequin number for Legendrian links in the topological link type K . Upper bounds on \overline{tb} in terms of other knot

invariants come from the following inequalities, where we abuse notation and use K to denote both a Legendrian link and its underlying topological link:

- $tb(K) + |r(K)| \leq 2g(K) - 1$, Bennequin's original result [2], where g is the genus of K ;
- $tb(K) + |r(K)| \leq 2g_4(K) - 1$ [23], where g_4 is the slice genus of K ;
- $tb(K) + |r(K)| \leq \min\text{-deg}_a H_K(a, z) - 1$ [8, 16], where H_K is the HOM-FLYPT polynomial and $\min\text{-deg}_a$ is the minimum degree in the variable a ;
- $tb(K) + |r(K)| \leq 2\tau(K) - 1$ [19], where $\tau(K)$ is the concordance invariant from knot Floer homology [18];
- $tb(K) + |r(K)| \leq s(K) - 1$ [20, 27], where $s(K)$ is Rasmussen's s -invariant [21];
- $tb(K) + |r(K)| \leq \hat{g}_{\min}(K)$ [29], where $\hat{g}_{\min}(K)$ is the minimal k such that the Khovanov–Rozansky cohomology $HKR_{k,l}^j(K)$ [12] is nonvanishing for some j, l ;
- $tb(K) \leq \min\text{-deg}_a F_K(a, z) - 1$ [22], where F_K is the Kauffman polynomial.

See [7] for further history (up to 2002). In the first six bounds, $r(K)$ is the rotation number of Legendrian K . Note that $r(K)$ is present in the first six bounds because they in fact bound the self-linking number of a transverse link. Any bound on $tb + |r|$ from transverse knot theory is fundamentally different from a direct bound on tb such as the Kauffman bound above. For instance, the maximal value for $tb + |r|$ for a left handed trefoil is -5 ; no bound on $tb + |r|$ can give the sharp result $\overline{tb} = -6$ in this case.

It is thus not surprising that the Kauffman bound tends to be more effective in bounding \overline{tb} for Legendrian links than the other bounds. The Kauffman bound is sharp (i.e., equality is attained) for two-bridge links, and for all but two knots with crossing number at most 9 [17]. It is, however, not sharp for many negative torus knots, for which \overline{tb} has been computed by Etnyre and Honda [6] using symplectic-topological techniques.

In this paper, we establish a new bound for \overline{tb} in terms of $(\mathfrak{sl}(2))$ Khovanov homology [11]. This bound is sharp for all alternating links, as well as all knots with crossing number at most 9, and all but at most two 10-crossing knots. In general, it seems to give the best overall currently known bound on \overline{tb} , although it is still not sharp for many negative torus knots, and occasionally gives a worse bound than Kauffman.

Recall that Khovanov homology associates to any oriented link K a bigraded abelian group $HKh^{*,*}(K)$, where the first grading is called the quantum (or Jones) grading and the second is the homological grading. If we disregard torsion, we obtain a two-variable Poincaré polynomial

$$Kh_K(q, t) = \sum \dim_{\mathbb{Q}}(HKh^{i,j}(K) \otimes \mathbb{Q})q^i t^j.$$

Khovanov homology is designed so that its graded Euler characteristic is the Jones polynomial $V_K: Kh_K(q, -1) = (q + q^{-1})V_K(q^2)$.

Theorem 1 (strong Khovanov bound) *For any link K ,*

$$\overline{tb}(K) \leq \min\{k \mid \bigoplus_{i-j=k} HKh^{i,j}(K) \neq 0\}.$$

Corollary 2 (weak Khovanov bound) $\overline{tb}(K) \leq \text{min-deg}_q Kh_K(q, t/q)$.

Theorem 1 and Corollary 2 often give the same bound on \overline{tb} , but there are instances in which Theorem 1 is stronger; see Section 4. We may deduce from the Khovanov bound another proof of the Legendrian corollary of the s -invariant bound above:

Corollary 3 *If K is a knot, then $\overline{tb}(K) \leq s(K) - 1$.*

Note that Corollary 3, in turn, implies the slice Bennequin bound $\overline{tb}(K) \leq 2g_4(K) - 1$; however, it is generally nowhere as effective as the Khovanov bound in bounding \overline{tb} .

By using the Khovanov bound, we can calculate \overline{tb} for alternating links.

Theorem 4 *The Khovanov bound (either weak or strong) is sharp for alternating links. If K is alternating and nonsplit, and $V_K(t), \sigma(K)$ are the Jones polynomial and signature of K respectively, then*

$$\overline{tb}(K) = \text{min-deg}_q V_K(q) + \sigma(K)/2 - 1.$$

Here we use the convention that the signature of the right handed trefoil is +2.

The reader may have noticed that the grading collapse in the strong Khovanov bound is the same as the one which Seidel and Smith use in their construction of a link invariant from Lagrangian intersection Floer homology [25]. Indeed, it is likely that one could bound $\overline{tb}(K)$ above by the minimum degree in which Seidel–Smith’s “symplectic Khovanov cohomology” $HKh_{sym}^*(K)$ does

not vanish. (Here K might need to be replaced by its mirror, depending on conventions.) This would use unpublished work of Lipshitz and Manolescu constructing generators for symplectic Khovanov cohomology in terms of a bridge diagram of a link, generalizing [15]. However, such an upper bound would also follow from the strong Khovanov bound, if, as proposed in [25], there is a spectral sequence from HKh to HKh_{symp} ; in particular, Seidel–Smith’s conjecture that $HKh_{\text{symp}}^k(K) \cong \bigoplus_{i-j=k} HKh^{i,j}(K)$ would imply that the two bounds are actually identical.

We prove Theorem 1 in Section 2. The method of proof, which uses induction, seems to be somewhat different from the proofs of previous Thurston–Bennequin bounds. In particular, it yields a sufficient condition for a front to maximize tb , which can then be applied to calculate \overline{tb} for alternating knots and nonsplit links. The construction of maximal- tb fronts for alternating links requires some graph theory which is the subject of Section 3. We examine the Khovanov bound in some other illustrative examples in Section 4.

Acknowledgments I thank Robert Lipshitz and Ciprian Manolescu for useful discussions. This work is supported by a Five-Year Fellowship from the American Institute of Mathematics.

2 The Khovanov bound

This section contains the proof of Theorem 1 and some immediate applications.

We first review a bit of Legendrian knot theory. A generic Legendrian link in standard contact \mathbb{R}^3 projects in the xz plane to a *front*, whose only singularities are double points and semicubical cusps, and which has no vertical tangencies. A front can be resolved into a link diagram, which we call the “desingularization” of the front, by smoothing the cusps and turning each double point into a crossing in which the strand of more negative slope is the overstrand: $\times \rightarrow \times$. For an oriented front F , let $w(F)$ denote the writhe of the desingularization of F , and $c(F)$ half the number of cusps of F ; then the Thurston–Bennequin number of F is given by $tb(F) = w(F) - c(F)$.

Via desingularization, any front F has a Khovanov complex $CKh(F)$ whose homology is Khovanov homology. This complex is bigraded, but in this section (except for the proof of Corollary 3) we will collapse one direction of the grading and consider the single grading given by the quantum (q) grading minus the homological (t) grading: $|\mathbf{v}| = p(\mathbf{v}) + w(F)$. Here \mathbf{v} is a tensor product of

vectors \mathbf{v}_\pm , one associated to each component of a resolution of the desingularization of F , and p is defined by setting $p(\mathbf{v}_\pm) = \pm 1$. With respect to this grading, the homology $HKh^*(F)$ of $CKh^*(F)$ is an invariant of the link type of the desingularized front.

We will be primarily concerned with a shifted version CKh_{sh} of the Khovanov complex, with the grading given by $|\mathbf{v}'| = p(\mathbf{v})$. Note that $CKh_{sh}(F)$ and its homology $HKh_{sh}(F)$ do not depend on an orientation of F , and that $HKh^*(F) = HKh_{sh}^{*-w(F)}(F)$.

Proposition 5 $HKh_{sh}^*(F) = 0$ for $* < -c(F)$, and thus $HKh^*(F) = 0$ for $* < tb(F)$.

Theorem 1 follows immediately from Proposition 5. We will prove Proposition 5 by induction on the number of double points of F . First we need to introduce a bit of terminology.

We say that a front F is n -vanishing if $HKh_{sh}^*(F) = 0$ for $* < n$; Proposition 5 states that any front is $-c(F)$ -vanishing. Given an unoriented front F and a double point p in F , we can construct two new fronts $\text{Res}_0(F, p), \text{Res}_1(F, p)$ which, in the desingularized picture, are Khovanov’s 0, 1-resolutions of F at the crossing p ; that is, $\text{Res}_0(F, p)$ and $\text{Res}_1(F, p)$ are the fronts obtained from F by replacing the double point \times at p by \frown and \succ , respectively. Note that $c(F) = c(\text{Res}_0(F, p)) = c(\text{Res}_1(F, p)) - 1$.

Lemma 6 *There is a long exact sequence*

$$\begin{array}{ccc}
 HKh_{sh}(\text{Res}_0(F, p)) & \xrightarrow{(-1)} & HKh_{sh}(\text{Res}_1(F, p)) \\
 & \swarrow & \searrow \\
 & HKh_{sh}(F), &
 \end{array}$$

where the top map lowers degree by 1 and the other maps preserve degree.

Proof This follows directly from the short exact sequence of complexes

$$0 \rightarrow CKh_{sh}(\text{Res}_1(F, p)) \rightarrow CKh_{sh}(F) \rightarrow CKh_{sh}(\text{Res}_0(F, p)) \rightarrow 0,$$

which itself follows from the facts that $CKh_{sh}(F)$ without its differential is the direct sum $CKh_{sh}(\text{Res}_0(F, p)) \oplus CKh_{sh}(\text{Res}_1(F, p))$, and its differential preserves $CKh_{sh}(\text{Res}_1(F, p))$. □

Lemma 7 *If $\text{Res}_0(F, p)$ and $\text{Res}_1(F, p)$ are n -vanishing for some n , then so is F .*

Proof Immediate from the exactness of $HKh_{\text{sh}}^*(\text{Res}_1(F, p)) \rightarrow HKh_{\text{sh}}^*(F) \rightarrow HKh_{\text{sh}}^*(\text{Res}_0(F, p))$ from Lemma 6. \square

Proof of Proposition 5 We induct on the number of double points of F . If F has no double points, then it is an unlinked union of n unknots, where $n \leq c(F)$. An unknot has HKh^* supported in dimensions -1 and 1 , and so $HKh^*(F)$ is supported in dimensions between $-n$ and n ; since $w(F) = 0$, it follows that F is $-n$ -vanishing and hence $-c(F)$ -vanishing.

Now consider an arbitrary front F . Let p be the double point of F farthest to the right. We consider two cases.

If the two strands emanating from the right of p meet at a right cusp (i.e., p is part of a “fish”), then the desingularization of F is the same as the desingularization of $\text{Res}_0(F, p)$ except for the addition of a negative kink. If we give F any orientation and $\text{Res}_0(F, p)$ the induced orientation, then $w(F) = w(\text{Res}_0(F, p)) - 1$, and invariance under (topological) Reidemeister move I implies that $HKh^*(F) = HKh^*(\text{Res}_0(F, p))$ for all $*$. Thus $HKh_{\text{sh}}^*(F) = HKh_{\text{sh}}^{*-1}(\text{Res}_0(F, p))$ for all $*$, and the induction assumption that $\text{Res}_0(F, p)$ is $-c(F)$ -vanishing shows that F is as well.

Otherwise, the two strands from the right of p do not end at the same cusp. By the induction assumption, $\text{Res}_0(F, p)$ is $-c(F)$ -vanishing, and thus the induction step follows from Lemma 7 if we can show that $\text{Res}_1(F, p)$ is also $-c(F)$ -vanishing.

In terms of singularities, $\text{Res}_1(F, p)$ replaces p by two cusps, a right cusp (opening to the left) and a left cusp (opening to the right). Starting at the left cusp, follow the front $\text{Res}_1(F, p)$ in either direction until the front passes to the left of p ; the result is a zigzag path including the left cusp which does not cross itself or the rest of the front. For consecutive cusps along this zigzag, measure the difference between the x coordinates of the cusps, and let c_1, c_2 be the consecutive cusps for which this difference is smallest. If we traverse the zigzag path in either direction, c_1 and c_2 must be traversed both downwards or both upwards by minimality. The zigzag between these two cusps comprises a “stabilization” which can be eliminated to obtain another front F' which agrees with $\text{Res}_1(F, p)$ outside of the stabilization; see Figure 1.

Clearly $\text{Res}_1(F, p)$ and F' have the same HKh_{sh} since they have the same front desingularization. But now $c(F') = c(\text{Res}_1(F, p)) - 1 = c(F)$; by the induction hypothesis, F' and thus $\text{Res}_1(F, p)$ is $-c(F)$ -vanishing, as desired. \square

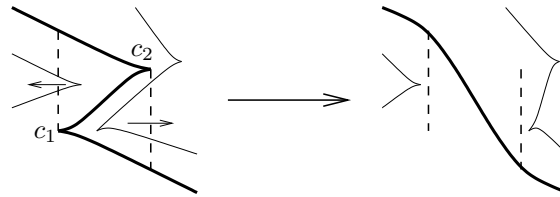


Figure 1: Eliminating cusps c_1 and c_2 . One may need to first perform an isotopy which pushes any part of the front with x coordinates between those of c_1 and c_2 out of the stabilization region.

The proof of Proposition 5 also yields a sufficient condition for a front to maximize tb in its topological class. Let the *0-resolution* of a front be the front which results from taking the 0-resolution of each double point: $\times \rightarrow \smile$. A 0-resolution is *admissible* if: (1) each component of the 0-resolution contains exactly two cusps; and (2) at each resolved double point, the two arcs of the resolution belong to different components of the 0-resolution.

Proposition 8 *Any front with admissible 0-resolution maximizes Thurston–Bennequin number in its topological link class; both weak and strong Khovanov bounds are sharp in this case.*

Proof Let F be a front with admissible 0-resolution. We wish to show that $HKh_{sh}^{-c(F)}(F)$ has positive free rank. Label the double points of F from left to right p_1, \dots, p_n , and let $F_0, F_1, \dots, F_n = F$ be the “partial 0-resolutions” obtained from F such that F_i is F but with 0-resolutions in place of p_{i+1}, \dots, p_n .

We prove by induction that $HKh_{sh}^{-c(F)}(F_i)$ has positive free rank for all i . For $i = 0$, F_0 is the 0-resolution of F , and by admissibility consists of $c(F)$ disjoint unknots; hence $HKh_{sh}^{-c(F)}(F_0) = \mathbb{Z}$.

Now suppose that $HKh_{sh}^{-c(F)}(F_{i-1})$ has positive free rank. By Lemma 6, we have an exact sequence

$$HKh_{sh}^{-c(F)}(F_i) \rightarrow HKh_{sh}^{-c(F)}(F_{i-1}) \rightarrow HKh_{sh}^{-c(F)-1}(\text{Res}_1(F_i, p_i)).$$

By admissibility, the two strands emanating to the right of p_i in F_i do not meet at a cusp, and so the proof of Proposition 5 implies that $\text{Res}_1(F_i, p_i)$ is $-c(F)$ -vanishing. Thus $HKh_{sh}^{-c(F)}(F_i) \rightarrow HKh_{sh}^{-c(F)}(F_{i-1})$ is a surjection, and the induction step is complete. \square

Proposition 8 immediately implies that the Khovanov bound is sharp for closures of positive braids, i.e., braids consisting of positive products of elementary

braid generators, with the convention that the right handed trefoil is the closure of a positive braid. Note that \overline{tb} was already known in this case, as Bennequin's original bound is sharp.

We remark that an admissible 0-resolution of a front constitutes an ungraded normal ruling (or proper decomposition) of the front in the sense of [4, 9]. It follows that the Chekanov–Eliashberg differential graded algebra [4] for the front has an augmentation, and in particular that the front is not Legendrian isotopic to a stabilization (i.e., a front with a small zigzag). Proposition 8 strengthens the result that the front is not destabilizable.

Note that since the original release of this paper, Rutherford [24] has obtained a significant generalization of Proposition 8: any front admitting an ungraded normal ruling maximizes Thurston–Bennequin number in its topological link class.

We will use Proposition 8 in Section 3 to calculate \overline{tb} for alternating links by showing that any alternating link has a front with admissible 0-resolution. It is not known what class of knots has a front with admissible 0-resolution; alternating links and closures of positive braids fall into this category, while links for which the Khovanov bound is not sharp (e.g., many negative torus knots) do not.

To conclude this section, we use the weak Khovanov bound to deduce the s -invariant bound on \overline{tb} .

Proof of Corollary 3 Recall the definition of the s -invariant from [21]: there is a spectral sequence from the bigraded Khovanov homology $HKh(K) \otimes \mathbb{Q}$ to another knot homology $HKh'(K)$ introduced by Lee [13], and $HKh'(K) = \mathbb{Q} \oplus \mathbb{Q}$ has a summand in each of quantum gradings $s(K) \pm 1$. Lee gives an explicit set of generators of $HKh'(K)$, called “canonical generators” in [21]; it is easy to see that both canonical generators have homological grading 0. It follows that $HKh'(K)$ and thus $HKh^{*,*}(K) \otimes \mathbb{Q}$ is nonzero in bidegree $(s(K) \pm 1, 0)$. Now apply the weak Khovanov bound. \square

3 Alternating links

In this section, we show that the Khovanov bound is sharp for alternating links. It is well known that there is a correspondence between alternating links and planar graphs. For our purposes, a planar graph is a graph embedded in the plane which may have more than one edge connecting a pair of vertices, but

has no edges connecting a vertex to itself. We consider planar graphs up to isotopies of the plane.

Definition 9 A *reduced planar graph* is a 1-connected planar graph; that is, it is connected and cannot be disconnected by removing one edge. In particular, it has no vertices of valence 1.

There is a standard way to obtain a reduced planar graph from a reduced alternating link diagram. (Recall that an alternating diagram is reduced if there is no crossing whose removal splits the diagram into two disjoint parts; any alternating link has a reduced alternating diagram.) Such a diagram divides the plane into a number of components; color these components in a checkerboard fashion so that near any crossing \times , the coloring takes the form \otimes . The vertices of the planar graph correspond to black regions, and the edges are diagram crossings where two black regions meet.

We will need another way to depict a planar graph.

Definition 10 A *Mondrian diagram* consists of a set of disjoint horizontal line segments in the plane, along with a set of disjoint vertical line segments, each of which begins and ends on a horizontal segment and does not intersect any other horizontal segment.

Any Mondrian diagram yields a planar graph by contracting the horizontal segments to points.

Proposition 11 *All reduced planar graphs are the contraction of some Mondrian diagram.*

In fact, Proposition 11 holds for arbitrary planar graphs; this generalization is easy to establish from Proposition 11, but we need only the reduced case for our purposes.

We delay the proof of Proposition 11 until the end of this section. First we apply it to the maximal Thurston–Bennequin number for alternating links.

Let K be an alternating link; this has a reduced alternating diagram which gives rise to a planar graph. Consider a Mondrian diagram whose contraction is this graph. If necessary, extend the ends of the horizontal segments of this diagram slightly so that no vertical segment ends at an endpoint of a horizontal segment. We can now turn this Mondrian diagram into a front as follows: replace each

horizontal segment by a “pair of lips” front for the unknot, and delete from these fronts a neighborhood of each intersection with a vertical segment; then replace each vertical segment by an X. This front represents a Legendrian link of the topological type of K . See Figure 2 for an example.

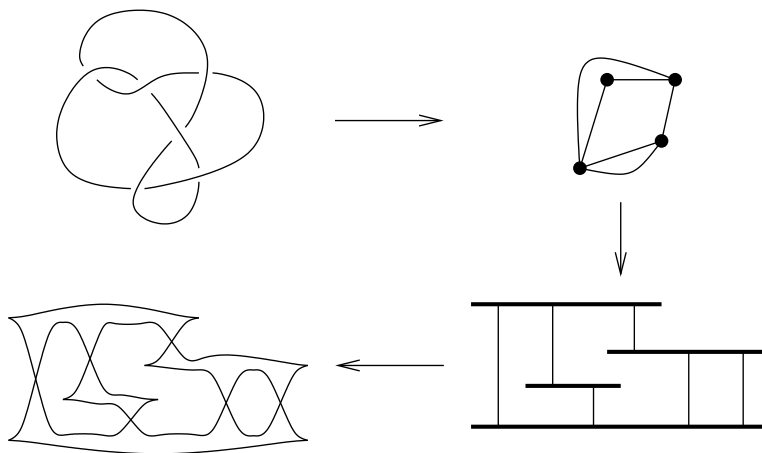


Figure 2: Using a Mondrian diagram to construct a Legendrian form for the knot 6_3 . Clockwise, from left: a reduced alternating diagram for 6_3 ; the corresponding planar graph; a Mondrian diagram contracting to this graph; a front for 6_3 .

We are now in a position to prove the sharpness of the Khovanov bound for alternating links.

Proof of Theorem 4 The fact that the weak (and hence also the strong) Khovanov bound is sharp for alternating knots follows from Proposition 8 and the observation that the front constructed above from a Mondrian diagram is admissible. To complete the proof of the proposition, we need to establish that $\min\text{-deg}_q Kh_K(q, t/q) = \min\text{-deg}_q V_K(q) + \sigma(K)/2 - 1$ for alternating nonsplit links K . This follows easily from the identity $Kh_K(q, -1) = (q + q^{-1})V_K(q^2)$, along with a result of Lee [13]:

$$Kh_K(q, t) = q^{\sigma(K)}(q^{-1} + q + (q^{-1} + tq^3)Kh'_K(tq^2)),$$

where Kh'_K is some Laurent polynomial. Note that our sign convention for σ is the opposite of Lee's. \square

We remark that, by work of Murasugi or Thistlethwaite, the expression from Theorem 4 for $\overline{tb}(K)$ when K is alternating and nonsplit can be rewritten as follows:

$$\overline{tb}(K) = -c_-(K) + \sigma(K) - 1,$$

where $c_-(K)$ is the number of negative crossings in any reduced alternating diagram for K . As another side note, Theorem 4, together with the fact that the Kauffman bound is also sharp for alternating links [24], implies that for K alternating,

$$\min\text{-deg}_q Kh_K(q, t/q) = \min\text{-deg}_a F_K(a, z) - 1,$$

where $F_K(a, z)$ is the Kauffman polynomial of K , normalized so that the Kauffman polynomial of the unknot is 1.

The rest of this section is devoted to a proof of Proposition 11. We will actually prove a slightly stronger statement. The complement of a Mondrian diagram in the plane consists of several connected components, one unbounded and the rest bounded. Call a bounded component *strong* if the interior R of its closure has the following property: there is a horizontal line segment L in R such that every nonempty vertical slice of R (the intersection of R with a vertical line) is connected and intersects L . In this case, L is called a *spine* of the region. See Figure 3. A Mondrian diagram is called strong if each bounded component of its complement is strong.

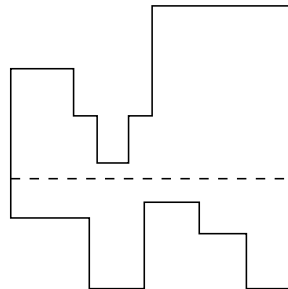


Figure 3: A strong region, with spine given by the dashed line. For an example of a strong Mondrian diagram, see Figure 2.

We will prove that any reduced planar graph is the contraction of a strong Mondrian diagram. Let G be a reduced planar graph; we construct a strong Mondrian diagram for G from the outside in.

Define the *boundary* of a planar graph to be the subgraph consisting of vertices and edges abutting the unbounded region in the complement of the graph. Call a planar graph an *enhanced cycle* if its boundary is a cycle (with no repeated vertices); an enhanced cycle consists of this cycle, along with some number of edges inside the cycle which connect vertices of the cycle.

We will construct strong Mondrian diagrams for a sequence of subgraphs of G which build up to G .

Step 1 Any planar cycle. Here a strong Mondrian diagram is given by a step-shaped construction as shown in Figure 4.

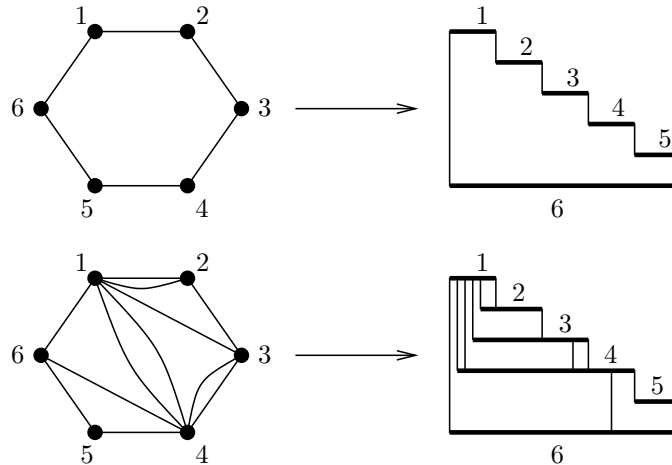


Figure 4: Step-shaped Mondrian diagram for a cycle (top), and resulting strong Mondrian diagram for an enhanced cycle (bottom)

Step 2 An enhanced cycle C . Number the vertices of C $1, \dots, n$ in clockwise order around the boundary cycle \tilde{C} . From the previous step, \tilde{C} is the contraction of a step-shaped Mondrian diagram whose “steps” from top to bottom correspond in order to $1, \dots, n$. There is now an essentially unique way to expand this Mondrian diagram to give one for C ; see Figure 4. More precisely, for an edge in $C \setminus \tilde{C}$ joining vertices i and j with $i < j$, drop a perpendicular from the step i to the level of j . Do this for each edge in $C \setminus \tilde{C}$, and arrange the perpendiculars so that the lengths of the perpendiculars dropped from any particular step i are nonincreasing as we view the perpendiculars from left to right. Now extend each step leftwards just as far as it needs to go to meet each perpendicular which ends at its height. The planarity of \tilde{C} implies that the resulting diagram is a Mondrian diagram; its strongness follows from the easily checked fact that each bounded region in its complement is step-shaped.

For the next steps, label the vertices of G v_1, \dots, v_m in such a way that v_1, \dots, v_k for some k are the vertices on the boundary of G , and the subgraph of G induced by v_1, \dots, v_l is connected for all $l \geq k$.

Step 3 The subgraph G_k of G induced by v_1, \dots, v_k . Since the boundary of G consists of an edge-disjoint union of cycles, G_k consists of an edge-disjoint

union of enhanced cycles, joined in treelike fashion by their common vertices. We can build a strong Mondrian diagram for G_k by starting with the strong Mondrian diagram for one of the enhanced cycles, extending rightward each horizontal segment corresponding to a vertex to which other enhanced cycles are attached, placing strong Mondrian diagrams for these attached enhanced cycles with base on the extended segments, and continuing in this fashion until all of G_k has been constructed. Here we use the fact that any vertex of an enhanced cycle can serve as the base of its step-shaped Mondrian diagram. See Figure 5 for a (probably clearer) pictorial example.

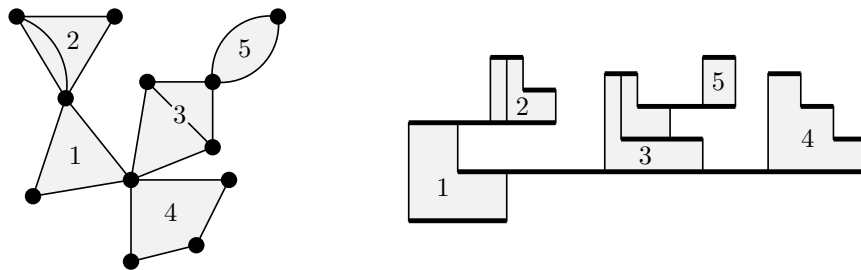


Figure 5: Joining Mondrian diagrams for enhanced cycles (labeled 1, 2, 3, 4, 5)

Step 4 The subgraph G_l of G induced by v_1, \dots, v_l , for $k < l \leq m$. This proceeds by induction on l . Assume that we have a strong Mondrian diagram which contracts to G_{l-1} ; we construct one for G_l . Note that G_l is G_{l-1} along with vertex v_l and the edges from v_l to G_{l-1} ; we may assume that there are at least two such edges, since if there is only one, we can double it and then remove the double at the end of the induction process.

Let R be the component of the complement of G_{l-1} which contains v_l , corresponding to a strong region \tilde{R} in the strong Mondrian diagram for G_{l-1} . Fix a spine of \tilde{R} . For each edge from v_l to a vertex on the boundary of R , locate the (unique) horizontal boundary component of \tilde{R} corresponding to this vertex, and drop a vertical perpendicular from this horizontal segment to the spine. We may assume that no two perpendiculars land on the same point of the spine. The subset of the spine beginning at the foot of the leftmost perpendicular and ending at the foot of the rightmost perpendicular will contract to the vertex v_l . See Figure 6.

The Mondrian diagram for G_l now consists of the Mondrian diagram for G_{l-1} , along with this shortened spine and the perpendiculars to it. To see that it is strong, note that for each region into which \tilde{R} is split, a horizontal slice of the

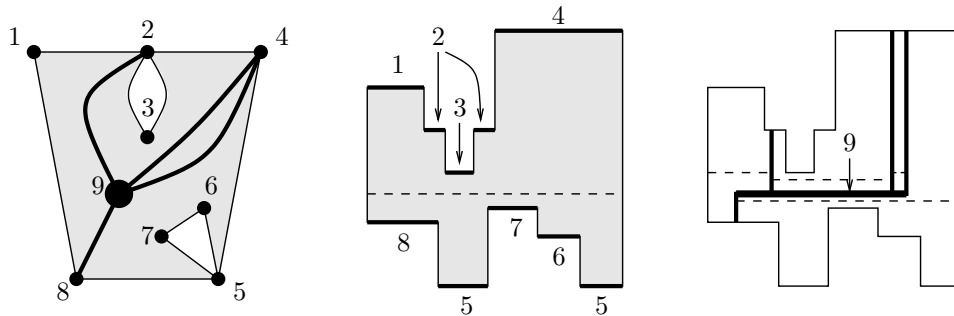


Figure 6: Induction step in the construction of a strong Mondrian diagram. We wish to add vertex 9 in the region R in the planar graph (left) to the region \tilde{R} in the Mondrian diagram (center). A portion of the spine (dashed line, center) becomes the horizontal segment corresponding to vertex 9. The result is the figure on the right (with spines for each region given by the dashed lines).

region either just above or just below the spine of \tilde{R} constitutes a spine for the region.

At the end of the induction for Step 4, we have a strong Mondrian diagram for G , possibly with some doubled edges. By removing the extraneous vertical segments corresponding to these doubled edges, we obtain a strong Mondrian diagram for G , as desired.

4 Computations

We now discuss various computations of the Khovanov bound, its sharpness, and its relation to other known bounds on \overline{tb} . We use the standard knot notation as shown in Rolfsen for knots with at most 10 crossings, and Dowker–Thistlethwaite notation for knots with 11 crossings, and denote mirroring by an overline; for instance, $11n_{24}$ denotes the 24th nonalternating 11-crossing knot in the Dowker–Thistlethwaite enumeration, and $\overline{11n_{24}}$ is its mirror. Many computations in this section were assisted by the program *Knotscape* [10], the *Mathematica* package *KnotTheory* [1], the online Table of Knot Invariants [14], and the Khovanov homology data of Shumakovitch [26].

The Khovanov bound (either strong or weak) is quite effective in calculating maximal Thurston–Bennequin number. It is sharp for all knots with 9 or fewer crossings, and in particular resolves the one unknown value in the table of \overline{tb} from [17].

Proposition 12 $\overline{tb}(\overline{9_{42}}) = -5$.

For 10-crossing knots, Theorem 4 allows us to restrict our attention to the 42 prime nonalternating knots and their mirrors. Hand-drawn front diagrams by the author (see the author’s web page for details) yield the following result.

Proposition 13 *The Khovanov bound (either strong or weak) is sharp for all knots with 10 or fewer crossings, with the exception of $\overline{10_{124}}$, for which $\overline{tb}(\overline{10_{124}}) = -15$ while the Khovanov bound is -14 , and the possible exception of $\overline{10_{132}}$, for which we have $-1 \leq \overline{tb}(\overline{10_{132}}) \leq 0$.*

For the negative torus knot $\overline{10_{124}} = T(5, -3)$, the computation of \overline{tb} comes from [6]. A diagram of $\overline{10_{132}}$ with $tb = -1$ is given in Figure 7, while the Khovanov bound is 0. A table of values for \overline{tb} for prime knots up to 10 crossings, deduced from Proposition 13, is available online at [14].

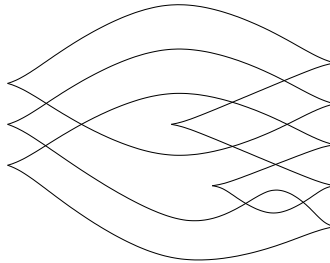


Figure 7: A possible maximal- tb representative for $\overline{10_{132}}$?

Negative torus knots provide a number of further examples of nonsharpness of the Khovanov bound. The Khovanov bound (strong or weak) is sharp for negative torus knots $T(2n + 1, -2)$, $T(4, -3)$, and $T(7, -5)$, but for no other examples where the author has computed it. We note that the Kauffman bound is sharp for $T(p, -q)$ when $p > q$ and q is even [5]; when $p > q$ and q is odd, it appears that the Khovanov bound gives a better estimate than Kauffman, though neither is sharp in general.

As a particular example, consider $T(5, -4)$. Here the strong and weak Khovanov bounds for $\overline{tb}(T(5, -4))$ are different,¹ given by -19 and -18 , respectively [28]; the difference is the torsion group $HKh^{-29, -10}(T(5, -4)) = \mathbb{Z}/2$. Here neither Khovanov bound is sharp, while the Kauffman bound does give the sharp value $\overline{tb} = -20$.

¹This seems to be a relatively unusual situation. There are no knots with crossing number 13 or less for which the strong and weak Khovanov bounds disagree.

We see from this example that the Khovanov and Kauffman bounds are incommensurate. However, for small knots at least, the Khovanov bound often seems to be better when the two disagree. There are 19 knots with 11 or fewer crossings for which the bounds disagree: $\overline{8}_{19}$, $\overline{9}_{42}$, $\overline{10}_{124}$, $\overline{10}_{128}$, $\overline{10}_{136}$, $\overline{11n}_{20}$, $\overline{11n}_{24}$, $\overline{11n}_{27}$, $\overline{11n}_{37}$, $\overline{11n}_{50}$, $\overline{11n}_{61}$, $\overline{11n}_{70}$, $\overline{11n}_{79}$, $\overline{11n}_{81}$, $\overline{11n}_{86}$, $\overline{11n}_{107}$, $\overline{11n}_{126}$, $\overline{11n}_{133}$, and $\overline{11n}_{138}$. For all of these, the Khovanov bound is better. Of the 46 12-crossing knots where the bounds disagree, Kauffman is better for one ($\overline{12n}_{475}$, also the only knot with 12 or fewer crossings for which the HOMFLYPT bound is stronger than Khovanov), and Khovanov is better for the rest.

References

- [1] **D Bar-Natan**, *The Mathematica package KnotTheory`*, available at: <http://katlas.math.toronto.edu/wiki/>
- [2] **D Bennequin**, *Entrelacements et équations de Pfaff*, from: “Third Schnepfenried geometry conference, Vol. 1 (Schnepfenried, 1982)”, Astérisque 107, Soc. Math. France, Paris (1983) 87–161 MR753131
- [3] **Y V Chekanov**, *Differential algebra of Legendrian links*, Invent. Math. 150 (2002) 441–483 MR1946550
- [4] **Y V Chekanov**, **P E Pushkar’**, *Combinatorics of fronts of Legendrian links, and the Arnol’d 4-conjectures*, Uspekhi Mat. Nauk 60 (2005) 99–154 MR2145660
- [5] **J Epstein**, **D Fuchs**, *On the invariants of Legendrian mirror torus links*, from: “Symplectic and contact topology: interactions and perspectives (Toronto, ON/Montreal, QC, 2001)”, Fields Inst. Commun. 35, Amer. Math. Soc., Providence, RI (2003) 103–115 MR1969270
- [6] **J B Etnyre**, **K Honda**, *Knots and contact geometry. I. Torus knots and the figure eight knot*, J. Symplectic Geom. 1 (2001) 63–120 MR1959579
- [7] **E Ferrand**, *On Legendrian knots and polynomial invariants*, Proc. Amer. Math. Soc. 130 (2002) 1169–1176 MR1873793
- [8] **J Franks**, **R F Williams**, *Braids and the Jones polynomial*, Trans. Amer. Math. Soc. 303 (1987) 97–108 MR896009
- [9] **D Fuchs**, *Chekanov-Eliashberg invariant of Legendrian knots: existence of augmentations*, J. Geom. Phys. 47 (2003) 43–65 MR1985483
- [10] **J Hoste**, **M Thistlethwaite**, *Knotscape*, available at: <http://www.math.utk.edu/~morwen/knotscape.html>
- [11] **M Khovanov**, *A categorification of the Jones polynomial*, Duke Math. J. 101 (2000) 359–426 MR1740682

- [12] **M Khovanov, L Rozansky**, *Matrix factorizations and link homology II*, arXiv:math.QA/0505056
- [13] **E S Lee**, *An endomorphism of the Khovanov invariant*, Adv. Math. 197 (2005) 554–586
- [14] **C Livingston, J C Cha**, *KnotInfo: Table of knot invariants*, available at: <http://www.indiana.edu/~knotinfo/>
- [15] **C Manolescu**, *Nilpotent slices, Hilbert schemes, and the Jones polynomial*, Duke Math. J. to appear
- [16] **H R Morton**, *Seifert circles and knot polynomials*, Math. Proc. Cambridge Philos. Soc. 99 (1986) 107–109 MR809504
- [17] **L L Ng**, *Maximal Thurston–Bennequin number of two-bridge links*, Algebr. Geom. Topol. 1 (2001) 427–434 MR1852765
- [18] **P Ozsváth, Z Szabó**, *Knot Floer homology and the four-ball genus*, Geom. Topol. 7 (2003) 615–639 MR2026543
- [19] **O Plamenevskaya**, *Bounds for the Thurston–Bennequin number from Floer homology*, Algebr. Geom. Topol. 4 (2004) 399–406 MR2077671
- [20] **O Plamenevskaya**, *Transverse knots and Khovanov homology*, e-print (2004) arXiv:math.GT/0412184
- [21] **J Rasmussen**, *Khovanov homology and the slice genus*, e-print (2004) arXiv:math.GT/0402131
- [22] **L Rudolph**, *A congruence between link polynomials*, Math. Proc. Cambridge Philos. Soc. 107 (1990) 319–327 MR1027784
- [23] **L Rudolph**, *Quasipositivity as an obstruction to sliceness*, Bull. Amer. Math. Soc. (N.S.) 29 (1993) 51–59 MR1193540
- [24] **D Rutherford**, *The Bennequin number, Kauffman polynomial, and ruling invariants of a Legendrian link: the Fuchs conjecture and beyond*, arXiv:math.GT/0511097
- [25] **P Seidel, I Smith**, *A link invariant from the symplectic geometry of nilpotent slices*, arXiv:math.SG/0405089
- [26] **A Shumakovitch**, *KhoHo*, available at <http://www.geometrie.ch/KhoHo/>
- [27] **A Shumakovitch**, *Rasmussen invariant, slice–Bennequin inequality, and sliceness of knots*, arXiv:math.GT/0411643
- [28] **A Shumakovitch**, *Torsion of the Khovanov homology*, e-print (2004) arXiv:math.GT/0405474
- [29] **H Wu**, *Braids and the Khovanov–Rozansky cohomology*, e-print (2005) arXiv:math.GT/0508064

Department of Mathematics, Stanford University, Stanford, CA 94305, USA

Email: lng@math.stanford.edu

URL: <http://alum.mit.edu/www/ng>

Received: 16 September 2005